2018 European Control Conference (ECC)
June 12-15, 2018. Limassol, Cyprus

Human-Robot Collaboration based on Robust Motion Intention Estimation with Prescribed Performance

Christos N. Mavridis[1], Konstantinos Alevizos[2], Charalampos P. Bechlioulis[2] and Kostas J. Kyriakopoulos[2]

Abstract— **This paper addresses the problem of physical human-robot collaboration for object manipulation. In particular, we consider a human-robot architecture where the human has exclusive knowledge of the object's desired trajectory and the robot tries to assist actively, by carrying the object's load in order to reduce the human effort that is required to achieve the desired tracking behavior. The robot estimates the human's desired motion via a prescribed performance estimation law that drives the estimation error to an arbitrarily small residual set. This estimation is further employed in the object dynamics equation to compute the interaction force between the human and the object. Subsequently, an impedance control scheme is designed based on the aforementioned estimations, achieving significant reduction on the required human effort, despite the uncertainty in the robot dynamics. The feedback relies exclusively on the robot's force/torque, position as well as velocity measurements and no a priori explicit information on the task is required. Finally, extensive experimental results clarify the proposed method and verify its efficiency.**

I. Introduction

As robots are advancing in both industry and everyday life, physical human-robot interaction gains increasing interest in robotic research. Various assistive and rehabilitation robotic technologies have emerged that relieve patients in their daily tasks, whereas robots and human workers, sharing a common workspace, interact physically and collaborate. This paper concentrates on cooperative object manipulation for human and robotic co-workers carrying out transportation tasks that were previously impossible for either the human or the robot alone. In this way, the combination of the robot's power and the human's planning and decision-making capabilities will result in a powerful and versatile technology for industry.

A lot of research has been conducted in this field with the first results pertaining to passive systems. As shown in [1], [2], such systems cooperate well with humans via physical interaction, although they lack the ability to minimize the human effort and actively contribute to the transportation task. As a result, researchers came up with various proactive systems to address the problem of cooperative object manipulation. In [3], [4], encountering the concept of role assignment, novel strategies have been developed for effort sharing. However, this is only applicable when the desired trajectory is a priori known, which rarely is the case in non-structured environments. Other proactive systems rely on methods based on human motion intention estimation combined with an indirect force control scheme. In [5], for a simple transportation task with known starting and ending points, a Kalman filter is used to estimate the parameters of the well-known minimum jerk profile. Afterwards, the results are fed in an admittance and impedance control scheme respectively. In the same spirit, a neural network was trained in [6] to predict human motion intention taking as inputs position, velocity and force measurements. The predicted trajectory is then provided to an adaptive impedance controller.

To tackle the cooperative object manipulation problem and particularly the aspects discussed above, various techniques that rely on task-specific learning and programming-by-demonstration have also been proposed. In [7], reinforcement learning and extended Kalman filtering are combined to develop a behavior based gain controller that provides a weighted sum action of a reactive and a proactive controller based on the confidence level prediction. In [8], hidden Markov models are applied to detect interaction patterns and classify them on the basis of a database and/or human rating. The proposed admittance controller acts as a passive system in case there is no clue for the interaction pattern, otherwise a motion is created and then translated to a virtual force profile. Programming-by-demonstration techniques are presented in [9]–[11]. In [9] a statistical model, based on Gaussian mixture models, is trained in a pure leader-follower role distribution after a set of demonstrations, and then the task is reproduced using Gaussian mixture regression. Observing the trajectory and interaction forces during demonstration tasks in [10], a Gaussian mixture model is employed to estimate the task parameters. The developed model is then able to generate the required force and trajectory profiles for similar cooperative tasks.

This paper addresses the motion intention estimation problem via a robust prescribed performance estimation law that drives the error between the actual and the desired trajectory estimation to an arbitrarily small residual set. The proposed method is based only on position and velocity measurements as well as the interaction force/torque measurements between the robot and the object. In this respect, the interaction force/torque between the human and the object, which is unknown and thus cannot be employed in the control design, is estimated using the object dynamics and the desired trajectory estimation. Subsequently, based on the aforementioned estimation strategy, an adaptive impedance control scheme

[1]Department of Electrical and Computer Engineering and Institute for Systems Research, University of Maryland, College Park, MD 20742, U.S.A. Email: mavridis@umd.edu.

[2]Control Systems Lab, School of Mechanical Engineering, National Technical University of Athens, 9 Heroon Polytechniou Str, Athens, 15780, Greece. Emails: kos.alevizos@gmail.com, chmpechl@mail.ntua.gr, kkyria@mail.ntua.gr.

This work was supported by the EU funded project Co4Robots: Achieving Complex Collaborative Missions via Decentralized Control and Coordination of Interacting Robots, H2020-ICT-731869, 2017-2019.

is designed that leads to human's effort reduction through the impedance characteristics imposed to the system by the controller, despite the uncertainties in the robot dynamics.

In this work, we extend significantly the current state of art [12]–[14], via a more robust estimation algorithm that converges even though the desired object's acceleration profile is nonzero (i.e., arbitrary object's desired trajectory based on the human motion planning, as long as it is bounded and smooth). Moreover, the customizable ultimate bounds allow us to achieve practical stabilization of the tracking error, with accuracy limited only by the sensors' resolution. Finally, we increase the closed loop robustness by incorporating parametric uncertainty in the robot dynamics.

II. Problem formulation

In this paper, a typical human-robot collaboration system is investigated that involves a human limb and a robotic manipulator in a leader-follower scheme, handling a rigidly grasped object. It is assumed that the robotic manipulator has at least 6 degrees of freedom (DoF), is fully actuated, and is equipped with a force sensing handle at its end-effector, so that measurements of position, velocity and interaction forces/torques with the object are available. Furthermore, the geometric and inertial parameters of the grasped object are considered known. The object's desired trajectory profile $x_{dl}(t)$ is determined by the human-leader, whereas the robot-follower estimates it by $x_{df}(t)$ via its own available sensing. The human partner leads the task by simply applying forces to the object, while the robot control objective is to achieve "active" following by carrying the object's load, thus reducing the interaction force between the human and the object.

A. Kinematics

We denote the human's hand coordinates (leader) and the robot's task space coordinates (follower) with respect to an inertial frame $\{I\}$ by $x_i = \left[x_{ip}^T, x_{ir}^T\right]^T$, $i \in \{l, f\}$, where x_{ip} corresponds to the position and x_{ir} corresponds to the orientation expressed as roll, pitch and yaw angles. Similarly, we denote the object's coordinates with respect to $\{I\}$ by $x_o = \left[x_{op}^T, x_{or}^T\right]^T$. Assuming that the contacts are considered rigid, the following kinematic constraints hold:

$$x_{ip} = x_{op} + l_i \;\;\&\;\; x_{ir} = x_{or} + a_i,\; i \in \{l, f\} \qquad (1)$$

where the vectors $l_i = [l_{ix}, l_{iy}, l_{iz}]^T$ and $a_i = [a_{ix}, a_{iy}, a_{iz}]^T$ represent the fixed relation between the object's and the hand's/end-effector's frames expressed in $\{I\}$. Since the object's geometric parameters are considered known, the object's coordinates may be computed via (1). Furthermore, by differentiating (1) we establish the velocity relationships $\dot{x}_{ip} = \dot{x}_{op} + \dot{x}_{ir} \times l_i$, $\dot{x}_{ir} = \dot{x}_{or}$ or in a compact matrix form:

$$\dot{x}_i = J_{oi}\dot{x}_o = \begin{bmatrix} I_{3\times3} & -L_i \\ 0_{3\times3} & I_{3\times3} \end{bmatrix} \dot{x}_o,\; i \in \{l, f\} \qquad (2)$$

where J_{oi} is the Jacobian from the hand/end-effector to the object's center of mass and $L_i = \begin{bmatrix} 0 & -l_{iz} & l_{iy} \\ l_{iz} & 0 & -l_{ix} \\ -l_{iy} & l_{ix} & 0 \end{bmatrix}$ denotes the cross-product matrix. Notice that since the hand/end-effector and the object are rigidly connected, the aforementioned Jacobian is always full rank and hence a well-defined inverse J_{oi}^{-1} exists. Differentiating once more with respect to time, we also establish the acceleration relation:

$$\ddot{x}_i = \dot{J}_{oi}\dot{x}_o + J_{oi}\ddot{x}_o,\; i \in \{l, f\}. \qquad (3)$$

Moreover, let q_f be the joint space variables of the robot. Invoking the forward kinematics, we express the task space variables as a nonlinear function of the joint variables as $x_f = F_f(q_f)$. Finally, differentiating the above equation, we obtain $\dot{x}_f = J_f(q_f)\,\dot{q}_f$, where $J_f(q_f) = \frac{\partial F_f(q_f)}{\partial q_f}$ is the Jacobian matrix.

B. Robot Dynamics

The dynamic model of the robot, in terms of task space coordinates, is described by:

$$M_r(q_f)\,\ddot{x}_f + C_r(\dot{q}_f, q_f)\,\dot{x}_f + G_r(q_f) = U_f + F_f \qquad (4)$$

where M_f is the positive definite inertial matrix, C_f is a matrix that models Coriolis and centrifugal effects and G_f represents gravitational forces. The term F_f involves the interaction force/torque exerted at the end effector by the object and U_f denotes the input task space wrench. The relation between the joint torques τ_f and the task space wrench is given by $\tau_f = \overline{J}_f^T U_f + \left(I - J_f^T \overline{J}_f^T\right)\tau_{in}$, where $\overline{J}_f$ is the generalized inverse that is consistent with the equations of motion of the manipulator and its end-effector [15]. The vector τ_{in} does not contribute to the end-effector's wrench and can be regulated independently to achieve secondary goals (e.g., manipulability increase or collision avoidance for the links).

Finally, invoking the kinematic relations (1)-(3), we may express the aforementioned dynamic model (4) with respect to the object's coordinates as follows:

$$M_{of}(q_f)\,\ddot{x}_o + C_{of}(\dot{q}_f, q_f)\,\dot{x}_o + G_{of}(q_f) = J_{of}^T U_f + J_{of}^T F_f \qquad (5)$$

where

$$\begin{aligned} M_{of}(q_f) &= J_{of}^T M_f(q_f)\, J_{of} \\ C_{of}(\dot{q}_f, q_f) &= J_{of}^T (C_f(\dot{q}_f, q_f)\, J_{of} + M_f(q_f)\,\dot{J}_{of}) \\ G_{of}(q_f) &= J_{of}^T G_f(q_f) \end{aligned}$$

and the following properties hold true.

Property 1: The inertial matrix $M_{of}(q_f)$ is symmetric and positive definite.

Property 2: The matrix $2C_{of}(q_f, \dot{q}_f) - \dot{M}_{of}(q_f)$ is skew-symmetric, i.e., $\xi^T(2C_{of}(q_f, \dot{q}_f) - \dot{M}_{of}(q_f))\xi = 0, \forall \xi \in \mathbb{R}^6$.

Property 3: The physical parameters of the robot appear linearly in the dynamic model (5) in terms of a set of unknown but constant parameter vector $\theta \in \Re^Q$ as follows:

$$M_{of}(a)d + C_{of}(b, a)c + G_{of}(a) = Y(a, b, c, d)\theta$$

where $Y(a, b, c, d)$ is a $6 \times Q$ regressor matrix, composed of smooth and known nonlinear functions.

C. Human Limb Model

A generic model that describes the dynamics of a human limb during the execution of a movement involves a mass-damper-spring property, as in [16]:

$$M_l\left(\ddot{x}_{dl}-\ddot{x}_l\right)+C_l\left(\dot{x}_{dl}-\dot{x}_l\right)+G_l\left(x_{dl}-x_l\right)=F_h \quad (6)$$

where M_l, C_l, and G_l are the unknown mass, damper, and spring matrices of the human limb, respectively, and $\ddot{x}_{dl}$, $\dot{x}_{dl}$, and, x_{dl} form the trajectory of the human's hand, planned in the human subject's central nervous system. The term F_h represents the force exerted by the human limb on the object, which tends to zero when the actual trajectory converges to the desired one.

Similarly to the robot's case, we may express the aforementioned dynamic model (6) with respect to the object's coordinates, invoking the kinematic relations (1)-(3), as follows:

$$M_{ol}\left(\ddot{x}_{dl}-\ddot{x}_o\right)+C_{ol}\left(\dot{x}_{dl}-\dot{x}_o\right)+G_{ol}\left(x_{dl}-x_o\right)=-J_{ol}^T F_l \quad (7)$$

where $F_l=-F_h$ represents the force exerted on the human's limb, J_{ol} is the Jacobian from the human's hand to the object's center of mass (2), and the unknown matrices M_{ol}, C_{ol}, G_{ol} are expressed in the same way as in (5).

D. Object Dynamics

Under the assumption that the commonly grasped object is rigid (i.e., no deformations take place under the action of the applied forces by the human and the robot) the following rigid body dynamics holds:

$$M_o(x_o)\ddot{x}_o+C_o(x_o,\dot{x}_o)\dot{x}_o+G_o=F_o \quad (8)$$

where M_o, C_o, G_o model the inertial, coriolis and gravity effects and the force F_o exerted on the object is computed as:

$$F_o=-J_{ol}^T F_l-J_{of}^T F_f=-GF \quad (9)$$

with $G=\left[J_{ol}^T,J_{of}^T\right]$ denoting the grasp matrix of the overall configuration and $F=\left[F_l^T,F_f^T\right]^T$.

E. Problem Statement

In a conventional robot task, the desired trajectory is a priori known and available in the control design. Alternatively, in a multi-robot system under a leader-follower architecture with known robot dynamics, the desired trajectory, which was known exclusively to the leader, could be implicitly conveyed to the followers as in [17]. However, in a human-robot collaboration task, the desired trajectory is exclusively determined by the human and thus cannot be considered in the robot control design. Therefore, an estimate x_{df} of the desired trajectory profile at the follower's side should first be designed and subsequently an impedance control approach should be adopted such that the robot arm is controlled to be compliant to the force exerted by the human. Consequently, considering the force exerted on the object (8)-(9) by the human, the robot arm dynamics with respect to the object's coordinates (5) should be governed by an impedance model:

$$M_d(\ddot{x}_o-\ddot{x}_{df})+C_d(\dot{x}_o-\dot{x}_{df})+G_d(x_o-x_{df})=-J_{ol}^T F_l \quad (10)$$

where M_d, C_d, G_d are the desired inertia, damping, and stiffness matrices, respectively.

III. Control Methodology

The aforementioned desired impedance model suggests that the actual position of the object x_o is refined according to the interaction force $-J_{ol}^T F_l$. Equivalently, the human will feel like moving an object with inertia M_d, damping C_d, and stiffness G_d. In this paper, x_{df} will be designed to change according to the motion intention of the human through an appropriately selected robust estimation law to be described in the sequel. Subsequently, an adaptive control scheme will be developed to impose the desired impedance model (10), despite the uncertainty in the robot dynamics.

A. Estimation law

In order to achieve the desired impedance behaviour, the estimation law should not only estimate the object's desired trajectory profile $x_{dl}(t)$, but also compensate for acceleration residuals, since acceleration measurements are not available. In this respect, we relax the specification on asymptotic estimation by adopting a robust prescribed performance estimator that guarantees ultimate boundedness of the estimation error $e(t)=x_o(t)-x_{df}(t)$. The mathematical representation of prescribed performance for each element of $e(t)=\left[e_1(t),e_2(t),\ldots\right]^T$ is given by the following inequalities:

$$-\rho_j(t)<e_j(t)<\rho_j(t),\ \forall t\geq 0 \quad (11)$$

where $\rho_j(t)$ denotes the corresponding performance function that encapsulates the desired transient and steady state performance specifications (e.g., convergence rate, maximum steady state error). A candidate exponential performance function may be defined by:

$$\rho_j(t)=(\rho_{j,0}-\rho_{j,\infty})e^{-st}+\rho_{j,\infty} \quad (12)$$

where the constant s dictates the exponential convergence rate, $\rho_{j,\infty}$ denotes the ultimate bound at the steady state and $\rho_{j,0}$ is chosen to satisfy $\rho_{jo}>|e_j(0)|$. Hence, following the prescribed performance control methodology [18], the estimation law is designed as follows:

$$\dot{x}_{dfj}=k_j\ln\left(\frac{1+\frac{e_j(t)}{\rho_j(t)}}{1-\frac{e_j(t)}{\rho_j(t)}}\right)-\frac{e_j(t)}{\rho_j(t)}\dot{\rho}_j(t),\ k_j>0 \quad (13)$$

from which the follower's estimate $x_{dfj}(t)$ is calculated via a simple integration. Moreover, we may calculate the desired acceleration signal by:

$$\ddot{x}_{dfj}=\left(\frac{2k_j}{1-\left(\frac{e_j(t)}{\rho_j(t)}\right)^2}-\dot{\rho}_j(t)\right)\frac{\dot{e}_j(t)\rho_j(t)-e_j(t)\dot{\rho}_j(t)}{\rho_j^2(t)}-\frac{e_j(t)}{\rho_j(t)}\ddot{\rho}_j(t) \quad (14)$$

by simply differentiating (13). with respect to time

Theorem 1: Consider the error $e(t) = x_o(t) - x_{df}(t)$, where $x_o(t)$ and $x_{df}(t)$ denote the object's actual position/orientation and the estimate of the desired trajectory at the follower's side respectively. Given a smooth and bounded desired trajectory $x_{dl}(t)$ with bounded derivatives as well as the appropriately selected performance functions $\rho_j(t)$ for each element of $e(t) = [e_1(t), e_2(t), \dots]^T$ that satisfy $|e_j(0)| < \rho_j(0)$ and incorporate the desired transient and steady state performance specifications, the estimation law (13) guarantees that $|e_j(t)| < \rho_j(t)$, $\forall t \geq 0$.

Proof: The proof follows identical arguments for each element of $e(t)$. Hence, let us define the normalized error:

$$\xi_j = \frac{e_j(t)}{\rho_j(t)}. \tag{15}$$

The estimation law (13) may be rewritten as a function of the normalized error ξ_j as follows:

$$\dot{x}_{dfj} = k_j \ln\left(\frac{1+\xi_j}{1-\xi_j}\right) - \xi_j \dot{\rho}_j(t). \tag{16}$$

Differentiating ξ_j with respect to time and substituting (16), we obtain:

$$\dot{\xi}_j = h_j(t, \xi_j) = \frac{\dot{x}_{oj}(t) - k_j \ln\left(\frac{1+\xi_j}{1-\xi_j}\right)}{\rho_j(t)}. \tag{17}$$

We also define the non-empty and open set $\Omega_{\xi_j} = (-1, 1)$. In the sequel, we shall prove that $\xi_j(t)$ never escapes a compact subset of Ω_{ξ_j} and thus the performance bounds (11) are met. The following analysis is divided in two phases. First, we show that a maximal solution exists, such that $\xi_j(t) \in \Omega_{\xi_j}$ $\forall t \in [0, \tau_{\max})$, and subsequently we prove by contradiction that $\tau_{\max}$ is extended to ∞.

Phase A: Since $|e_j(0)| < \rho_j(0)$, we conclude that $\xi_j(0) \in \Omega_{\xi_j}$. Additionally, owing to the smoothness of: a) the object's trajectory and b) the proposed estimation scheme (13) over Ω_{ξ_j}, the function $h_j(t, \xi_j)$ is continuous for all $t \geq 0$ and $\xi_j \in \Omega_{\xi_j}$. Therefore, the hypotheses of Theorem 54 (pp.476) in [19] hold and the existence of a maximal solution $\xi_j(t)$ of (17) on a time interval $[0, \tau_{\max})$ such that $\xi_j(t) \in \Omega_{\xi_j}$, $\forall t \in [0, \tau_{\max})$ is ensured.

Phase B: Notice that the transformed error signal:

$$\varepsilon_j(t) = \ln\left(\frac{1+\xi_j(t)}{1-\xi_j(t)}\right) \tag{18}$$

is well defined for all $t \in [0, \tau_{\max})$. Hence, consider the positive definite and radially unbounded function $V_j = \frac{1}{2}\varepsilon_j^2$. Differentiating with respect to time and substituting (17), we obtain:

$$\dot{V}_j = \frac{2\varepsilon_j}{(1-\xi_j^2)\rho_j(t)}\left(\dot{x}_{oj}(t) - k_j \varepsilon_j\right) \tag{19}$$

Owing to the fact that $\frac{1}{1-\xi_j^2} > 1, \forall \xi_j \in \Omega_{\xi_j}$, $\rho_j(t) > 0, \forall t \geq 0$, and $|\dot{x}_{oj}(t)|$ is assumed bounded by an unknown positive constant $\bar{U}_j$, we conclude that $\dot{V}_j < 0$ when $|\varepsilon_j(t)| > \frac{\bar{U}_j}{k_j}$ and consequently that:

$$|\varepsilon_j(t)| \leq \bar{\varepsilon}_j = \max\left\{|\varepsilon_j(0)|, \frac{\bar{U}_j}{k_j}\right\}, \forall t \in [0, \tau_{\max}). \tag{20}$$

Thus, invoking the inverse of (18), we get:

$$-1 < \frac{e^{-\bar{\varepsilon}_j} - 1}{e^{-\bar{\varepsilon}_j} + 1} = \underline{\xi}_j \leq \xi_j(t) \leq \overline{\xi}_j = \frac{e^{\bar{\varepsilon}_j} - 1}{e^{\bar{\varepsilon}_j} + 1} < 1. \tag{21}$$

Therefore, $\xi_j(t) \in \Omega'_{\xi_j} = \left[\underline{\xi}_j, \overline{\xi}_j\right]$, $\forall t \in [0, \tau_{\max})$, which is a nonempty and compact subset of Ω_{ξ_j}. Hence, assuming $\tau_{\max} < \infty$ and since $\Omega'_{\xi_j} \subset \Omega_{\xi_j}$, Proposition C.3.6 (pp. 481) in [19] dictates the existence of a time instance $t' \in [0, \tau_{\max})$ such that $\xi_j\left(t'\right) \notin \Omega'_{\xi_j}$, which is a clear contradiction. Therefore, $\tau_{\max}$ is extended to ∞. As a result, all closed loop signals remain bounded and moreover $\xi_j(t) \in \Omega'_{\xi_j} \subset \Omega_{\xi_j}$, $\forall t \geq 0$. Finally, from (15) and (21), we conclude that:

$$-\rho_j(t) < \underline{\xi}_j \rho_j(t) \leq e_j(t) \leq \overline{\xi}_j \rho_j(t) < \rho_j(t)$$

for all $t \geq 0$, which completes the proof. ■

Remark 1: The proposed estimation scheme is more robust against desired trajectory profiles with non-zero acceleration than previous works presented in [12]–[14]. The only necessary condition concerns the smoothness and boundedness of the desired trajectory. In this sense, our method guarantees bounded closed loop signals and practical asymptotic stabilization of the estimation errors.

B. Adaptive Impedance Control

Let us define the error $e(t) = x_o(t) - x_{df}(t)$, where x_{df}, $\dot{x}_{df}$, and $\ddot{x}_{df}$ are calculated by (13) and (14). In this subsection, we design an adaptive control scheme to impose the desired impedance model (10) on the robot dynamics (5). Thus, the control objective is to enforce $\lim_{t\to\infty} w(t) = 0$, where the error signal $w(t)$ is constructed as $w = M_d\ddot{e} + C_d\dot{e} + G_d e + J_{ol}^T F_l$. However, since the interaction force $F_{ho} = -J_{ol}^T F_l$ between the human and the object is not available to the robot, we exploit: a) the ultimate boundedness of the tracking error $e(t) = x_o(t) - x_{df}(t)$, b) the inertial and geometric parameters of the object, which are assumed known, as well as c) the dynamic equation of the object (8), to estimate it by:

$$\hat{F}_{ho} = M_o\ddot{x}_{df} + C_o(x_o, \dot{x}_o)\dot{x}_o + G_o + J_{of}^T F_f$$

Equivalently, invoking (8), we obtain:

$$\begin{aligned} -J_{ol}^T F_l &= M_o\ddot{x}_o + C_o(x_o, \dot{x}_o)\dot{x}_o + G_o + J_{of}^T F_f \\ &= M_o\ddot{x}_{df} + C_o(x_o, \dot{x}_o)\dot{x}_o + G_o + J_{of}^T F_f + M_o\ddot{e} \\ &= \hat{F}_{ho} + M_o\ddot{e} \end{aligned}$$

Thus, selecting M_d such that $M_d^* = M_d - M_o$ is positive definite, the error signal w becomes:

$$w = M_d^*\ddot{e} + C_d\dot{e} + G_d e - \hat{F}_{ho}$$

and consequently we get an augmented impedance error:

$$\bar{w} = K_f w = \ddot{e} + K_d\dot{e} + K_p e - K_f\hat{F}_{ho} \tag{22}$$

where $K_f = M_d^{*-1}$, $K_p = K_f G_d$, and $K_d = K_f C_d$. We also choose two positive-definite matrices Λ and Γ such that $\Lambda + \Gamma = K_d$ and $\dot{\Lambda} + \Gamma\Lambda = K_p$ and we define the filtered force measurement $\dot{f}_l + \Gamma f_l = K_f\hat{F}_{ho}$. Thus, we may rewrite (22) as $\bar{w} = \ddot{e} + (\Lambda + \Gamma)\dot{e} + (\dot{\Lambda} + \Gamma\Lambda)e - \dot{f}_l - \Gamma f_l$. Similarly to [6], we define the auxiliary variable z as:

$$z = \dot{e} + \Lambda e - f_l. \tag{23}$$

Hence, the augmented impedance error becomes:

$$\bar{w} = \dot{z} + \Gamma z \tag{24}$$

which is a stable low pass filter. Therefore, if we achieve $\lim_{t\to\infty} z(t) = 0$, then the initial control objective is readily met, i.e., $\lim_{t\to\infty} w(t) = 0$. In this respect, let us define the augmented reference variable:

$$\dot{x}_r = \dot{x}_{df} - \Lambda e + f_l. \tag{25}$$

Hence, (23) and (25) immediately result in:

$$z = \dot{x}_o - \dot{x}_r \tag{26}$$

from which (5) becomes:

$$M_{of}\dot{z} + C_{of} z = J_{of}^T U_f + J_{of}^T F_f - \left(M_{of}\ddot{x}_r + C_{of}\dot{x}_r + G_{of}\right).$$

Finally, invoking Property 3, we arrive at the open loop dynamics:

$$M_{of}\dot{z} + C_{of} z = J_{of}^T U_f + J_{of}^T F_f - Y(q_f, \dot{q}_f, \dot{x}_r, \ddot{x}_r)\theta. \tag{27}$$

Therefore, we design the following impedance control scheme:

$$U_f = -F_f + J_{of}^{-T}\left(Y(q_f, \dot{q}_f, \dot{x}_r, \ddot{x}_r)\hat{\theta} - Kz\right) \tag{28}$$

where $K > 0$ is a positive definite gain matrix and the estimate $\hat{\theta}$ of the unknown parameters θ are provided by the update law:

$$\dot{\hat{\theta}} = -\gamma Y^T(q_f, \dot{q}_f, \dot{x}_r, \ddot{x}_r) z \tag{29}$$

with $\gamma > 0$.

Theorem 2: Consider the robot dynamics (4) and the desired impedance model (10). The control scheme (28) with the adaptive law (29) guarantees $\lim_{t\to\infty} z(t) = 0$ and the boundedness of all signals in the closed loop system.

Proof: Consider the following Lyapunov function candidate:

$$V = \frac{1}{2} z^T M_{of} z + \frac{1}{2\gamma}\tilde{\theta}^T\tilde{\theta},$$

where $\tilde{\theta} = \hat{\theta} - \theta$ denotes the parametric error. Differentiating with respect to time we obtain:

$$\dot{V} = \frac{1}{2} z^T \dot{M}_{of} z + z^T M_{of}\dot{z} + \frac{1}{\gamma}\tilde{\theta}^T\dot{\hat{\theta}}.$$

Invoking Property 2 and substituting the adaptive law (29) and the control law (28) in the dynamics (27), we get:

$$\dot{V} = -z^T K z \leq 0 \tag{30}$$

Hence, we deduce $z, \tilde{\theta} \in L_\infty$. Moreover, from the definition of z in (23), we conclude that $x_o, \dot{x}_o \in L_\infty$, and consequently $\dot{x}_r, \ddot{x}_r \in L_\infty$. Furthermore, employing (27), we arrive at $\dot{z} \in L_\infty$. Therefore, integrating both sides of (30) leads to

$$V(t) - V(0) \leq -\int_0^t z^T(\tau) K z(\tau) d\tau \tag{31}$$

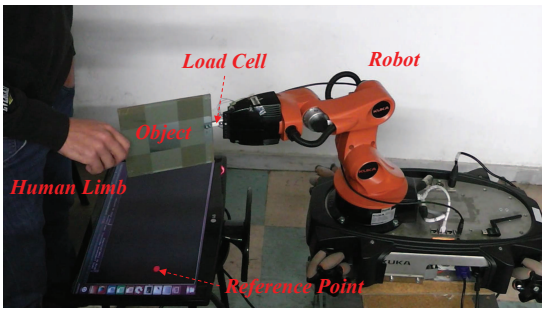

Fig. 1. The experimental setup.

Thus, $\int_0^t z^T(\tau) K z(\tau) d\tau$ is bounded, which results in $z \in L_2$. Finally, Barbalat's Lemma leads to $z \to 0$ as $t \to \infty$, since $z \in L_2$ and $\dot{z} \in L_\infty$, which completes the proof. ■

Remark 2: It should be noted that the only information needed on-line to implement the developed scheme concerns the measurements acquired exclusively by the robot's sensor suite (i.e., force, position and velocity). Regarding the control parameter tuning notice that $\rho_{j,\infty}$ can be set arbitrarily small to a value reflecting the resolution of the measurement device, thus achieving practical convergence of the estimation and tracking errors to zero. Moreover, the transient response of the estimation depends on both the convergence rate of the performance functions $\rho_j(t)$, that is directly affected by the parameter s, as well as the impedance control gain matrix K in (28).

IV. Experiments

The experimental evaluation of the proposed method was carried out in one degree of freedom using a KUKA youBot arm manipulator. Specifically, the manipulator was initialized in the configuration shown in Fig.1 and was kept fixed during the experiments. Only the motion of the first (base) joint was considered under torque control mode. A Phidgets micro load cell (0-780g) was mounted between the end effector and the object in order to measure the interaction force. Throughout the experiment, four subjects were asked to move the object keeping track of a reference trajectory that was displayed on a monitor below the manipulator (see Fig.1). The experiment was carried out 5 times at 3 different speed profiles (slow, normal, fast) for each subject. It should be noted that the reference trajectories were chosen according to the minimum-jerk profile to maintain a resemblance with the physical human motion. Finally, the parameters of the proposed scheme were selected as $M_d^\star = 0.01, G_d = 0.1, C_d = 0.2, K = 0.9, \gamma = 0.1$ and $\Lambda(0) = 0.5$.

The results revealed that all subjects were able to track the reference trajectory without difficulty and independently of the speed profile while the interaction with the object was entirely natural. The tracking response illustrated in Fig.2 is indicative of the method's performance. Notice however that the steady state position errors appear due to the fact that the subject's decision for the final position was influenced by the angle of view from above the monitor (see Fig.1). The statistical verification of the aforementioned statement

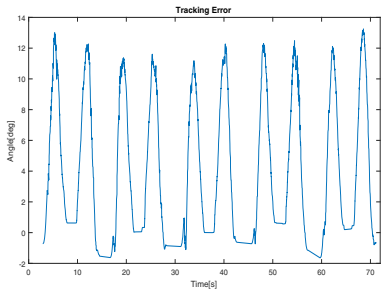

Fig. 2. The tracking error evolution for an indicative trial.

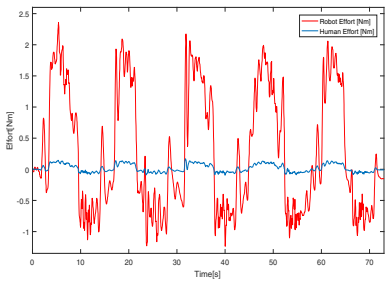

Fig. 3. The human and the robot effort for an indicative trial. Notice that the human is less than the robot effort for at least an order of magnitude

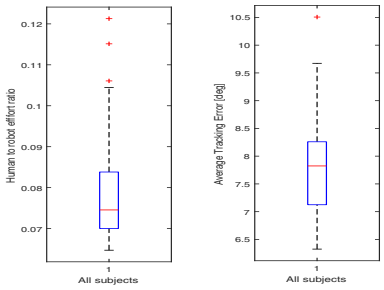

Fig. 4. The statistical illustration of the results for 4 subjects carrying out a tracking task 5 times for 3 different speed profiles (in total 60 trials).

in Fig.4 shows that the average absolute tracking error for all subjects and speed profiles has a mean value less than 8 degrees, which also encapsulates the human's tracking ability on a moving reference which in general is not negligible. In addition, the variance is around 0.78 indicating independence over different subjects and speed profiles.

The effort shared between the robot and the human is also effectively addressed. The human effort is reduced significantly over an order of magnitude compared to the robot's effort (see Fig.3). Notice that the statistical results of the human to robot effort ratio correspond to a mean value of 0.075 (more than an order of magnitude reduction) while the small variance confirms independence over subjects and speed profiles. Finally, a short video of the aforementioned experimental study can be found in https://vimeo.com/240159921.

V. Conclusions

In this work, a framework to deal with the emerging field of collaborative object manipulation through physical human-robot interaction is developed. A prescribed performance estimator was successfully employed for the motion intension estimation alongside with an adaptive impedance controller to drastically decrease the human's effort. The robot's position, velocity and force measurements consist the only sensing needed online for the controller's implementation. The experimental verification of the proposed method sets a new starting point for further research and extensive evaluation on mobile manipulator systems as well as multiple robotic agent scenarios.

References

[1] Y. Hirata, Y. Kume, Z. . Wang, and K. Kosuge, "Decentralized control of multiple mobile manipulators based on virtual 3-d caster motion for handling an object in cooperation with a human," in *Proceedings - IEEE International Conference on Robotics and Automation*, vol. 1, 2003, pp. 938–943.

[2] Y. Hirata and K. Kosuge, "Distributed robot helpers handling a single object in cooperation with a human," in *Proceedings - IEEE International Conference on Robotics and Automation*, vol. 1, 2000, pp. 458–463.

[3] A. Mrtl, M. Lawitzky, A. Kucukyilmaz, M. Sezgin, C. Basdogan, and S. Hirche, "The role of roles: Physical cooperation between humans and robots," *The International Journal of Robotics Research*, vol. 31, no. 13, pp. 1656–1674, 2012.

[4] Y. Li, S. Sam Ge, and C. Yang, "Learning impedance control for physical robot-environment interaction," *International Journal of Control*, vol. 85, no. 2, pp. 182–193, 2012.

[5] B. Corteville, E. Aertbelien, H. Bruyninckx, J. De Schutter, and H. Van Brussel, "Human-inspired robot assistant for fast point-to-point movements," in *Proceedings - IEEE International Conference on Robotics and Automation*, 2007, pp. 3639–3644.

[6] Y. Li and S. S. Ge, "Human-robot collaboration based on motion intention estimation," *IEEE/ASME Transactions on Mechatronics*, vol. 19, no. 3, pp. 1007–1014, 2014.

[7] A. Thobbi, Y. Gu, and W. Sheng, "Using human motion estimation for human-robot cooperative manipulation," in *IEEE International Conference on Intelligent Robots and Systems*, 2011, pp. 2873–2878.

[8] J. R. Medina, M. Lawitzky, A. Mrtl, D. Lee, and S. Hirche, "An experience-driven robotic assistant acquiring human knowledge to improve haptic cooperation," in *IEEE International Conference on Intelligent Robots and Systems*, 2011, pp. 2416–2422.

[9] P. Evrard, E. Gribovskaya, S. Calinon, A. Billard, and A. Kheddar, "Teaching physical collaborative tasks: Object-lifting case study with a humanoid," in *9th IEEE-RAS International Conference on Humanoid Robots, HUMANOIDS09*, 2009, pp. 399–404.

[10] L. Rozo, D. Bruno, S. Calinon, and D. G. Caldwell, "Learning optimal controllers in human-robot cooperative transportation tasks with position and force constraints," in *IEEE International Conference on Intelligent Robots and Systems*, vol. 2015-December, 2015, pp. 1024–1030.

[11] J. Dumora, F. Geffard, C. Bidard, N. A. Aspragathos, and P. Fraisse, "Robot assistance selection for large object manipulation with a human," in *Proceedings - 2013 IEEE International Conference on Systems, Man, and Cybernetics, SMC 2013*, 2013, pp. 1828–1833.

[12] K. Kosuge and T. Oosumi, "Decentralized control of multiple robots handling an object," in *Proceedings of the IEEE International Conference on Intelligent Robots and Systems*, vol. 1, 1996, pp. 318–323.

[13] K. Kosuge, T. Oosumi, and K. Chiba, "Load sharing of decentralized-controlled multiple mobile robots handling a single object," in *Proceedings of the IEEE International Conference on Robotics and Automation*, vol. 4, 1997, pp. 3373–3378.

[14] K. Kosuge, T. Oosumi, and H. Seki, "Decentralized control of multiple manipulators handling an object in coordination based on impedance control of each arm," in *Proceedings of the IEEE International Conference on Intelligent Robots and Systems*, vol. 1, 1997, pp. 17–22.

[15] O. Khatib, "Object manipulation in a multi-effector robot system," in *Proceedings of the 4th International Symposium on Robotics Research*, vol. 4. MIT Press, 1988, pp. 137–144.

[16] M. M. Rahman, R. Ikeura, and K. Mizutani, "Investigation of the impedance characteristic of human arm for development of robots to cooperate with humans," *JSME International Journal.Series C: Mechanical Systems, Machine Elements and Manufacturing*, vol. 45, no. 2, pp. 510–518, 2002.

[17] A. Tsiamis, C. K. Verginis, C. P. Bechlioulis, and K. J. Kyriakopoulos, "Cooperative manipulation exploiting only implicit communication," in *IEEE International Conference on Intelligent Robots and Systems*, vol. 2015-December, 2015, pp. 864–869.

[18] C. P. Bechlioulis and G. A. Rovithakis, "Robust partial-state feedback prescribed performance control of cascade systems with unknown nonlinearities," *IEEE Transactions on Automatic Control*, vol. 56, no. 9, pp. 2224–2230, 2011.

[19] E. D. Sontag, *Mathematical Control Theory*. London, U.K.: Springer, 1998.